

Spectral Lags Obtained by CCF of Smoothed Lightcurves

Li, Zhao-sheng, Chen Li, Wang, De-hua

Department of Astronomy, Beijing Normal University, Beijing, BJ 100875

chenli@bnu.edu.cn

ABSTRACT

We present a new technique to calculate the spectral lags of gamma-ray bursts (GRBs). Unlike previous processing methods, we first smooth the light curves of gamma-ray bursts in high and low energy bands using the “Loess” filter, then, we directly define the spectral lags as such to maximize the cross-correlation function (CCF) between two smoothed light curves. This method is suitable for various shapes of CCF; it effectively avoids the errors caused by manual selections for the fitting function and fitting interval. Using the method, we have carefully measured the spectral lags of individual pulses contained in BAT/Swift gamma-ray bursts with known redshifts, and confirmed the anti-correlation between the spectral lag and the isotropy luminosity. The distribution of spectral lags can be well fitted by four Gaussian components, with the centroids at 0.03 s, 0.09 s, 0.15 s, and 0.21 s, respectively. We find that some spectral lags of the multi-peak GRBs seem to evolve with time.

Subject headings: GRB; gamma ray bursts; spectral lag

1. Introduction

Observationally, the shape of a light curve of gamma-ray burst (GRB) is quite complex. It contains one or several pulses characterized by a fast rise followed by an exponential decay (FRED) profile (e.g., Fishman et al. 1994; Fenimore 1999). The majority of light curves do not present periodic variations. Light curves in different energy bands differ in many aspects, such as the widths. The widths of the pulses in the higher energy bands are usually smaller than those in the lower ones (Fenimore et al. 1995; Norris et al. 2005). The time delay among different energy photons is called spectral lag. As has been suspected, the spectral lags of GRBs and their evolution are vital for probing the physics of GRBs (Schaefer 2007). Lots of statistical works have been done (Band 1997; Norris et al. 2000; Chen et al. 2005). By using cross correlation function, Norris et al. (2000) estimated spectral lags of

six GRBs with known redshifts, concluding that the pulse peak luminosity and the spectral lag in time τ_{lag} are anticorrelated and can be well fitted with a power law $L \sim \tau_{\text{lag}}^{-1.14}$. Schaefer (2004) explained the relation and also demonstrated that the isotropic luminosity and the spectral lag should meet $L \sim \tau_{\text{lag}}^{-1}$. Shen et al. (2005) interpreted the spectral lag as the curvature effect of relativistic motion of GRB shells. Interestingly, Chen et al. (2005) examined the spectral lags of GRBs with multi-pulse, and found that there seemed to be no apparent correlation between spectral lags and luminosity in general for pulses within a given long GRB. Since Swift launched successfully, many GRBs have been measured redshifts (Gehrels, N. et al. 2004). With larger samples, this anti-correlation was checked carefully. The results show that the lag-luminosity correlation does exist, but with a larger scatter (Schaefer 2007; Xiao & Schaefer 2009; Ukwatta et al. 2010). The spectral lags in long and short GRBs are quite different. Generally, short GRBs have nearly zero lags and long GRBs have large positive lags (corresponding a temporal lead by higher energy γ -ray photons) (Band 1997). From this point of view, the spectral lags can be used as one of the observational parameters to classify the GRBs.

The procedure for estimating spectral lags of GRBs using a cross correlation function (CCF) has been widely adopted (e.g., Link et al. 1993; Fenimore et al. 1995; Norris et al. 2000). The CCF of $x_1(t)$ and $x_2(t)$ for a GRB, where $x_1(t)$ and $x_2(t)$ are the respective light curves in two different γ -ray photon energy bands, is simply defined as

$$\text{CCF}_{\text{Std}}(\tau; \nu_1, \nu_2) = \frac{\langle \nu_1(t + \tau) \nu_2(t) \rangle}{\sigma_{\nu_1} \sigma_{\nu_2}}, \quad (1)$$

where $\nu_i(t) \equiv x_i(t) - \langle x_i(t) \rangle$ is the light curve of zero mean and $\sigma_{\nu_i} = \langle \nu_i^2 \rangle^{1/2}$ is the standard deviation from the mean. The spectral lag τ_{lag} is defined as such that it maximizes $\text{CCF}(\tau; \nu_1, \nu_2)$. Because of the Poisson noise, τ_{lag} has to be evaluated through fitting the maximum of CCF with a polynomial function (Model I) or a Gaussian function with a linear term representing a background (Model II). For a faint burst, the CCF often displays asymmetry, or even multiple peaks. Therefore, using Model II to fit the CCF maximum will introduce a systematic bias. Whereas it is difficult to determine the degree of polynomial to fit CCF with model I. In both models, fitting interval of CCF will influence the result.

In order to reduce those man-made biases, we introduce a smooth technique. In Sec.2, we smooth the light curves of different energy bands with ‘‘Loess method’’, and then calculate the CCF of two smoothed curves, finally, we directly select the maximum point of CCF as the spectral lag. The Monto-Carlo simulation is implemented to confirm the smooth factor α . The algorithm looks simple and reasonable. In Sec.3, we apply this procedure to 121 GRBs detected by Swift and compare the results with traditional algorithm. The lag-luminosity correlation and lag-pulse width correlation are also carefully analyzed in the third section. At last, we analyze the results and give some brief discussions in section 4.

2. Procedure of Analysis

2.1. Smooth the Light Curves First

We use a moving loess (Cleveland 1979; Cleveland & Devlin 1988) filter to smooth the GRB light curves. The Loess filter is a local regression model, determined by only one parameter: the smoothing factor, α . α gives a percentage ($0 \leq \alpha \leq 1$), which means to take $\alpha \times 100$ % of the whole number of data as the smooth-span. For example, supposing a light curve contains 110 data points, x_1, \dots, x_{110} , taking $\alpha = 0.1$ then a smoothed value of x_8 is generated by a regression using linear least squares with 11 data points x_3, x_4, \dots, x_{13} and a 2nd degree polynomial model. Obviously, the α is smaller, the light curve is less smoothed, and vice versa. Especially, when $\alpha = 0$, no smooth has been applied. On the other hand, if α is too large, the smoothed light curve becomes very flat, i.e. $\alpha = 1$, the smooth-span is the interval of entire points. Fig. 1 displays the smoothing results of GRB 081222 with different α . It is easy to see that $\alpha = 0.2$ has stronger smoothing effect than $\alpha = 0.05$.

In this paper, the smoothing procedure is as follows: Suppose we have a single pulse GRB. First, we select an interval to cover the peak of the GRB light curve (e.g., T90, the duration over which a burst emits from 5% of its total fluence to 95%.) as time range for calculating spectral lag. Then, we choose an appropriate smooth factor α which is determined by Monto-Carlo simulations, taking each x_i as the center of its smoothing span. We then use a second order polynomial model to fit all data points in the span, and replace x_i by its fitted value. Obviously, this is a moving average filter.

Ukwatta et al. (2010) suggested that CCF_{Std} sometimes may not recover the artificial lag. So, in the paper, we adopt the CCF defined by Band (1997),

$$\text{CCF}_{x,y}(d) = \frac{\sum_{i=\max(1,1-d)}^{\min(N,N-d)} x_i y_{i+d}}{\sqrt{\sum_i x_i^2 \sum_i y_i^2}}. \quad (2)$$

Here, $x_i, y_i, i = 0, \dots, (N - 1)$ denote the data of respective smoothed light curves in two different energy bands. The spectral lag is defined by $\tau_{\text{lag}} = d \times t_b$, where d is the maximum of CCF, t_b is the size of a time-bin.

In order to determine a reasonable value of α , we calculated the lags between the simulated light-curves of high and low energy bands. We selected the following equation to model a pair of GRB light curves $F_h(t)$ (high energy band) and $F_l(t)$ (low energy band) (Abdo, A. A. et al. 2009):

$$F(t) = C_0 + p_0 \begin{cases} 0, t < t_0 \\ \frac{t-t_0}{\rho} \exp(-\frac{t-t_0}{\rho}), t > t_0, \end{cases} \quad (3)$$

where C_0 is the background counts rate, t_0 is the trigger time, p_0 and ρ represent the amplitude and the width of light curves respectively. Since our light curves were background-subtracted, therefore $C_0 = 0$. The observational facts tell us that the light curves of higher energy band have smaller p_0 and narrower width. In fact, the spectral lag obtained from the CCF has no relation to p_0 . So we just need to consider the width ratios between two energy bands. In this paper, we choose width ratios as 1.05. For a given width, we calculated the theoretical lags with equation (2). Then, we add a noise $X(t)$ on both $F_h(t)$ and $F_l(t)$, where $X(t)$ is a normally distributed random variable with expectation 0 and standard deviation σ . Obviously, a larger σ corresponds to a lower signal-to-noise ratio (S/N). By adjusting the value of σ , we obtain the light curves with different S/N from 5 to 10. After smoothing, we achieved the simulation spectral lags of noisy light curves. We shift alpha from 0.01 to 0.1 (step=0.01) to examine which α can fit the theoretical lags best. Fig. 2 illustrates the simulating results of “lag vs. α ”. Each panel of Fig. 2 contains a dashed line and 6 solid curves. The dashed line shows the value of the theoretical lag, while the rest of the solid curves are the lags obtained from 6 different S/N, with higher S/N indicating shorter error-bars. All the curves reveal a similar trend: the curves are mildly flattened and shows little bit spread; all simulated lags are very close to the theoretical lags. When α ranges between 0.05 and 0.1, the largest relative errors between simulated and theoretical lags are less than 5%. In order to simplify calculations, our samples take 0.1 and 0.05 as the smooth factor, respectively.

As a comparison, we perform the CCF for a pair of original light curves. In order to determine the maximum, we adopt Model II to calculate lags between the light curves:

$$f(t) = a \cdot \exp(-((t - b)/c)^2) + d \cdot t + e, \quad (4)$$

where a, b, c, d are fitting parameters. The spectral lag is $\tau_{\text{lag}} = t_{\text{max}} \times t_b$, where t_{max} represent the time corresponding to the maximum of $f(t)$, and t_b is the size of a time-bin.

2.2. Uncertainty Estimation

The Monte Carlo simulation is applied to estimate the uncertainty of spectral lags. For a pair of given light curves of high and low energy bands,

$$\begin{pmatrix} x_1, x_2, \dots, x_n \\ e_1, e_2, \dots, e_n \end{pmatrix} \text{ and } \begin{pmatrix} y_1, y_2, \dots, y_n \\ \varepsilon_1, \varepsilon_2, \dots, \varepsilon_n \end{pmatrix},$$

where, x_i and y_i are count rates of high and low energy bands, with measurement errors e_i and ε_i , respectively. Based on the data, we constructed a pair of simulated light curves

$(x'_1, x'_2, \dots, x'_n)$ and $(y'_1, y'_2, \dots, y'_n)$ by taking $x'_i \sim N(x_i, e_i^2)$ and $y'_i \sim N(y_i, \varepsilon_i^2)$, $i = 1, \dots, n$. Here, x'_i is a normally distributed random variable with expectation x_i and standard deviation e_i , $i = 1, \dots, n$. The explanation is similar to y'_i . In this work, we constructed 1000 (x'_i, y'_i) for each pair of observed x_i and y_i . We simulated 1000 light curves and derived the standard deviation of 1000 lags as the uncertainty estimate of the lag.

2.3. Determine the S/N and the duration of a GRB pulse

The ratio between the maximum of a pulse and the standard deviation of its background is defined as the S/N. Here the background is an interval taken before or after the pulse region. There are many works have been done to determine the duration of GRB (Scargle, J. D. 1998; Hakkila et al. 2003). In this work, we still use the smoothing skill. In Fig. 3, we utilize GRB 061007 as an example to represent the procedure of the duration of GRB pulses. We smooth the GRB light curve for energy band 15-150 keV with $\alpha = 0.1$. The smoothed light curve may contain a few local maximum values. The lags which the pulse peaks exceed 1σ background are returned. There are two ways to determine the width of individual pulse. First, when the pulse peak exists local minimums on both sides, the pulse duration is the interval between the local minimums. Second, when the pulse peak absents local minimum on one side (or both sides), we drew a horizontal line which height equals to the global minimum of smoothed light curve with 0.1σ background added, and then the intersection points between the horizontal line and the smoothed light curve are considered as start or end point of the pulse.

3. The GRBs sample and the results

3.1. Description of the GRBs sample

Since the successful launch of Swift satellite in November 2004 (Gehrels, N. et al. 2004), over 600 GRBs have been detected. Swift is a multi-wavelength satellite which can detect the gamma-ray transitional source and accurately locate the source within less than 100 seconds. Swift observations have played an inconceivably important role in GRB research.

The energy band of BAT/Swift is 15-350 keV. In practice, we only choose photons between 15 and 150 keV because the BAT is transparent to high energy photons over 150 keV. In previous works, GRBs light curves were extracted by specifying GRBs positions which were detected by BAT. Here, we use a slightly different method. The XRT can improve GRB position in both accuracy and precision by using the UVOT to accurately determine

Swift position (Goad et al. 2007; Evans et al. 2009). So, we apply enhanced XRT position to the procedure ‘batmaskwtevt’ and ‘batbinevt’ and extract background subtracted 15-25 keV and 50-100 keV light curves with a time bin size of 16 ms for spectral lag calculating.

Obviously, when we apply this procedure to a low S/N GRB, it can produce unendurable error. So, we select the GRBs with S/N larger than 5 in 15-25 keV energy range.

Our sample contains 121 long GRB detected by BAT/Swift from 2004 to 2010, 54 of them have measured redshifts.

3.2. Results

For a given spectral lag in advance, Ukwatta et al. (2010) simulated a group of light curves with the profile of a FRED pulse superposed on a background of different noise levels and fitted the peaks of CCF by a Gaussian function. The calculated lag was consistent with the value given previously. Through calculation we find that the CCF shows a symmetrical peak when the simulated light curves have FRED-like pulse shapes. Obviously, Gaussian curve is appropriate for fitting such maximum. The raw light curves, however, are much more complicated than the simulated ones, it is hard to get a good fitting with Gaussian function. As for our samples, the shapes of the CCF can be roughly classified into 3 categories: 1) Gaussian-like profile; 2) Asymmetric peak and 3) multi-peaks. Not difficult to imagine, it is easy to fit the first kind of CCF with a Gaussian function but hard for the other two kinds. We will compare the two methods with various shapes of CCF.

We choose GRB 080413B and GRB 071020 as examples. In Fig. 4, the CCF between 15-25 keV and 50-100 keV of GRB 080413B shows a Gaussian-like pulse. We fit the maximum of CCF with a Gaussian function plus a linear function and obtain the spectral lag and error, $\tau = 0.14 \pm 0.02$ s. Then, using the smooth method, we obtain $\tau = 0.14 \pm 0.02$ s. The results and figure show that either method can well model the spectral lag of GRB 080413B.

In Fig. 5, the CCF (circle) between 15-25 keV and 50-100 keV of GRB 071020 displays an asymmetry peak. There is an offset between A and B. If we change the fitting interval, point A will move, while the location of B is not related to the fitting interval. Although using a smaller fitting interval that contains the maximum of the CCF may yield similar lags, it will increase the lag uncertainty. Fig. 5 shows the smooth method (dashed line) is better for finding the maximum of CCF.

We list 121 spectral lags and pulse widths of GRBs in table 1 and table 2. For GRB with multiple pulses, we calculate each pulse of spectral lag. In the paper, the spectral lags

with smoothing factor $\alpha = 0.1$ and $\alpha = 0.05$ are utilized to analysis.

3.3. The Results Analysis

3.3.1. Comparison between Gaussian Curve Fitting and Smooth Method

From table 1 and table 2, we notice that the correlation coefficient between $\text{lag}_{\text{Gauss}}$ and $\text{lag}_{\text{loess}}$ is 0.9, which implies that the result of the two methods have high correlation. The $\text{lag}_{\text{Gauss}} - \text{lag}_{\text{loess}}$ relation is fitted by a linear function $\text{lag}_{\text{loess}}(s) = (0.75 \pm 0.05)\text{lag}_{\text{Gauss}}(s) + (0.005 \pm 0.03)$. Hence, the $\text{lag}_{\text{Gauss}}$ is systematically larger than $\text{lag}_{\text{loess}}$ by a factor of 4/3.

3.3.2. The Distribution of Spectral Lags With Smooth Method

Distribution of the lags can be obtained as follows: Assuming each spectral lag obeys a normal distribution with the mean equals to itself and the standard deviation equals to its uncertainty. In principle, the uncertainty of a lag should be larger than its temporal resolution, 0.016 s. Therefore, if a simulated uncertainty is smaller than 0.016 s, we set it to 0.016 s. In Fig. 7, we add all probability density function (PDF) together, and normalize the result. As seen in Fig. 7, the PDF of spectral lags has four components which locate at 0.028 ± 0.001 s, 0.091 ± 0.003 s, 0.151 ± 0.01 s, and 0.21 ± 0.01 s. Obviously, most of GRBs have positive spectral lags, which is consistent with the high energy photons arriving earlier than those with low energy photons in long GRBs.

3.3.3. The Relation between the Peak Isotropic Luminosity and the Lag of Primary Peak

Ukwatta et al. (2010) calculated spectral lags within the entire burst region for the “Gold sample” of GRBs detected by Swift, confirming the correlation between the peak isotropic luminosity and the lag of primary peak, albeit with a larger scatter in the relation. Hakkila et al. (2008) argued that it is reasonable to calculate individual pulse spectral lag instead of a burst range. From table 1 and table 2, our results support that each pulse spectral lag of multi-pulse GRBs has different delay time. We utilized spectrum and peak flux data from Bulter (2007) and Ukwatta et al. (2010), and tested the lag-pulse isotropic luminosity relation. Negative and zero lags were not shown in Fig. 8. The best fit is $\log L = (51.4 \pm 0.4) - (0.8 \pm 0.3) \log \text{lag}/(1+z)$. The correlation coefficient R equals to -0.6, and the slop (0.8 ± 0.3) cover the predicted slop of -1 by Schaefer (2004). Our results support

the lag-luminosity relation.

3.3.4. *The Lag-pulse Duration Relation*

Hakkila et al. (2008) reported a correlation between the spectral lag and pulse duration of GRBs with a high correlation coefficient ($R=0.97$), i.e., the shorter the duration of the pulse, the smaller the lag and the higher the luminosity and vice versa. We calculated the time duration and pulse spectral lag of each pulse in the samples. In Fig. 9, the lag-duration relation in the rest frame of GRBs is still establish but with a smaller correlation coefficient, $R=0.6$.

3.3.5. *The Evolution of the Lag with Time*

Most GRB light curves in the sample have multi-peak structure; we show the lag corresponding to each peak in table 1 and table 2. We find that different pulses in one GRB generally have different spectral lags, meaning that the lags evolve with time. Some GRBs (GRB 060927, GRB 061222A, GRB 080413A, GRB 080603B, GRB 090404, GRB 100615A) even have different signs from different pulses, i.e. during a multi-peak burst, one pulse has a positive lag, while the other may have a negative one. It may be due to the time evolution of peak energy which can produce negative lags (Peng, Z. Y., et al 2011; Ukwatta et al. 2011).

4. Conclusion

In this work, we develop a new method to calculate the spectral lags. Our method does not require the choose of fitting function and intervals, thus avoiding the human selection effects in traditional CCF fitting methods. The M-C simulation is utilized to determine the smooth factor α . The results show that our method obtains the introduced lags appropriately as long as taking α between 0.05 and 0.1. Using the method, we assign $\alpha = 0.05$ and $\alpha = 0.1$ to calculate the spectral lags of GRBs detected by Swift BAT, respectively. The Gaussian fitting and smoothing methods spectral lags list in table 1 and table 2. For two smoothing factors, most of spectral lags cover each other well. From Fig. 6, we see spectral lags fitted by Model II (i.e. Gauss+line) are strongly correlated with the smooth method results, that demonstrates our method is reasonable. It is worth noting that lags measured by our new method are systematically smaller than those calculated by traditional method. Figure 2 shows us that this is not caused by smoothing. We also verify the isotropic luminosity-

spectral lag relation, which is consistent with the work of Norris et al. (2000) and Ukwatta et al. (2010). By calculating multi-peak GRBs spectral lag, we find lags evolve with time with a weak tendency. Finally, Hakkila et al. (2008) reported the lag-pulse duration relation with an extremely high correlation coefficient. Our sample does not show this behavior.

We are grateful to the anonymous referee for a careful reading of this manuscript and for encouragement, constructive criticisms, valuable suggestions and helpful comments to improve the manuscript. We thank to Yuan Tiantian for careful reading and polishing the manuscript. This work has been supported by the National Science Foundation of China (NSFC 10778716, NSFC 11173024 and NSFC 10773034), National Basic Research program of China 973 Projects (2009CB824800) and the Fundamental Research Funds for the Central Universities. This work made use of data supplied by the UK Swift Science Data Centre at the University of Leicester.

REFERENCES

- Abdo. A. A., et al. 2009, *Nature*, Supplementary information, 331, 462
- Amati, L., et al. 2002, *A&A*, 390, 81
- Band, D. L. 1997, *ApJ*, 486, 928
- Bulter, N.R. et al. 2007, *ApJ*, 671,656
- Chen, L., Lou, Y.-Q., Wu, M., Qu, J.-L., Jia, S.-M., Yang, X.-J. 2005, *ApJ*, 619, 983
- Cheng, L. X., Ma, Y. Q., Cheng, K. S., Lu, T., Zhou, Y. Y. 1995, *A&A*, 300, 746
- Cleveland, W.S. 1979, *Journal of the American Statistical Association* 368, 829.
- Cleveland, W.S.; Devlin, S.J. 1988, *Journal of the American Statistical Association*, 403, 596.
- Evans et al. 2009, *MNRAS*, 397, 1177
- Fishman, G. J., et al. 1994, in *AIP Conf. Proc.* 307, *Gamma-Ray Bursts*, ed.G. J. Fishman (New York: AIP), 648
- Fenimore, E. E. 1999, *ApJ*, 518, 375
- Fenimore, E. E., Ramirez-Ruiz, E. [astro-ph/0004176\(2000\)](https://arxiv.org/abs/astro-ph/0004176)

- Fenimore, E. E., int Zand, J. J. M., Norris, J. P., Bonnell, J. T., Nemiroff, R. J. 1995, ApJ, 448, L101
- Gehrels, N., et al. 2004, ApJ, 611, 1005
- Goad et al. 2007, A&A, 476, 1401
- Hakkila, J., Giblin, T. W., Roiger, R. J., Haglin, D. J., Paciasas, W. S., Meegan, C. A. 2003, ApJ, 582, 320
- Hakkila, J., Giblin, T. W., Norris, J.P., Fragile, P.C., Bonnell, J.T. 2008, ApJ, 677, L81
- Link, B., Epstein, R. I., Friedhorsky, W. C. 1993, ApJ, 408, L81
- Norris, J. P., et al. 1996, ApJ, 459, 393
- Norris, J. P., Marani G. F., Bonnell J. T. 2000, ApJ, 534, 248
- 2005, Norris, J. P., et al. ApJ, 627, 324
- Peng, Z. Y., et al. Astronomische Nachrichten, 332, 92
- Reichart D. E. et al. 2000, ApJ, 552, 57
- Scargle, J. D. 1998, ApJ, 504, 405
- Schaefer, B. E. 2004, ApJ, 602, 306
- Schaefer, B. E. 2007, ApJ, 660, 16
- Rong-Feng Shen, Li-Ming Song, Zhuo Li. 2005, MNRAS, 362, 59
- Ukwatta, T. N., et al. 2010, ApJ, 711, 1073
- Ukwatta, T. N., et al. 2011, astro-ph/1109.0666v1(2011)
- Xiao L. M., Schaefer B. E. 2009, ApJ, 707, 387

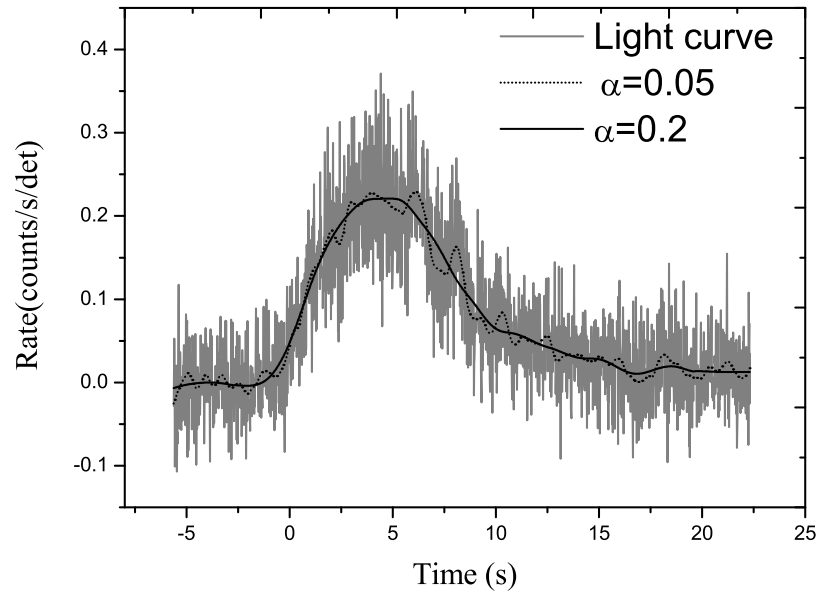


Fig. 1.— Light curve of GRB 081222 with a temporal resolution 16ms. The dotted and solid lines are the smoothed light curves with $\alpha = 0.05$ and $\alpha = 0.2$, respectively.

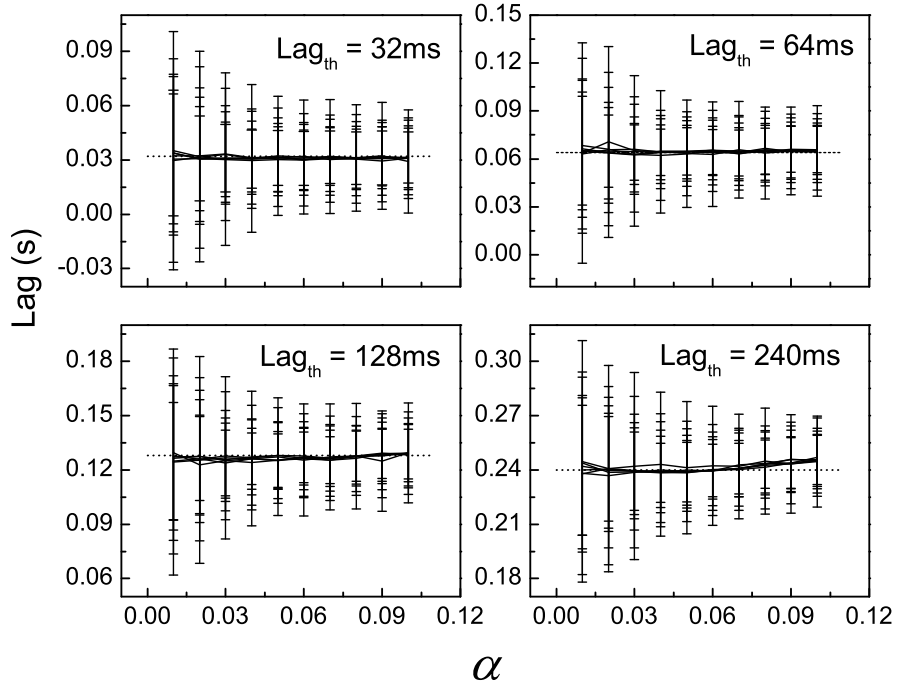


Fig. 2.— Lag vs. α . The width ratio is 1.05 and the theoretical lags are 32 ms, 64 ms, 128 ms and 240 ms, respectively. For each panel, the horizontal dotted line shows the theoretical lag. The horizontal axis represents α , and vertical axis represents lag. The spectral lags and corresponding error bars of light curves are displayed, with signal-to-noise changing from 5 to 10.

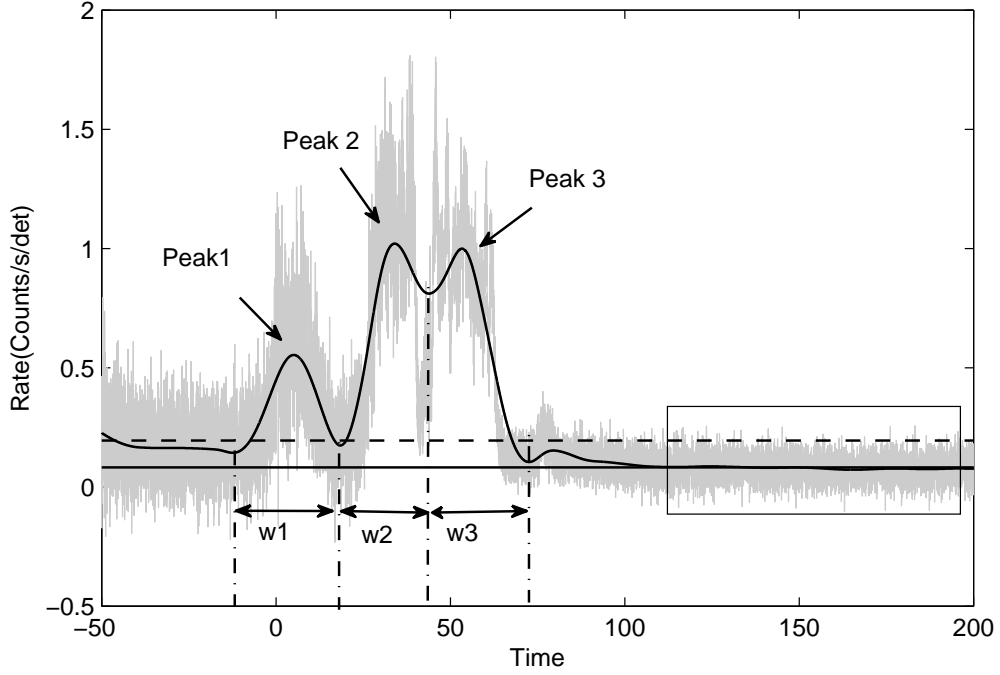


Fig. 3.— Determine the pulse duration of GRB. The rectangle region is considered as the GRB background, which standard derivation denotes as σ . The height of horizontal dashed line is minimum of smoothed light curve plus σ , only the local maximum of solid line above the dashed line are regarded as pulse. The vertical dot-dash lines represent the local minimums, and the pulse duration is the interval between two dot-dash lines (w_1 , w_2 , w_3 are the duration for three pulses). The height of horizontal solid line is the minimum of smoothed light curve plus 0.1σ . When the local maximum misses the local minimum on one side or both sides, the intersection points between the solid line and the smoothed light curve are considered as start or end time of the pulse.

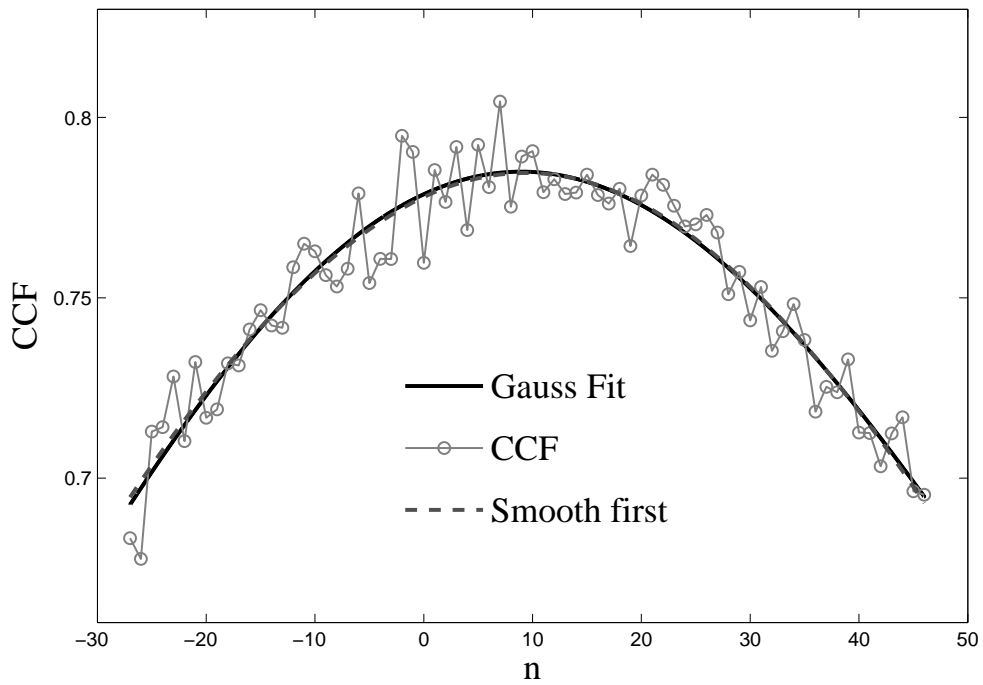


Fig. 4.— A comparison between Gaussian fitting and loess filter methods for GRB 080413B. The black points represent the CCF between 15-25 keV and 50-100 keV light curves. The solid and dashed lines represent the results fitted by traditional Gaussian fitting or smooth method, respectively.

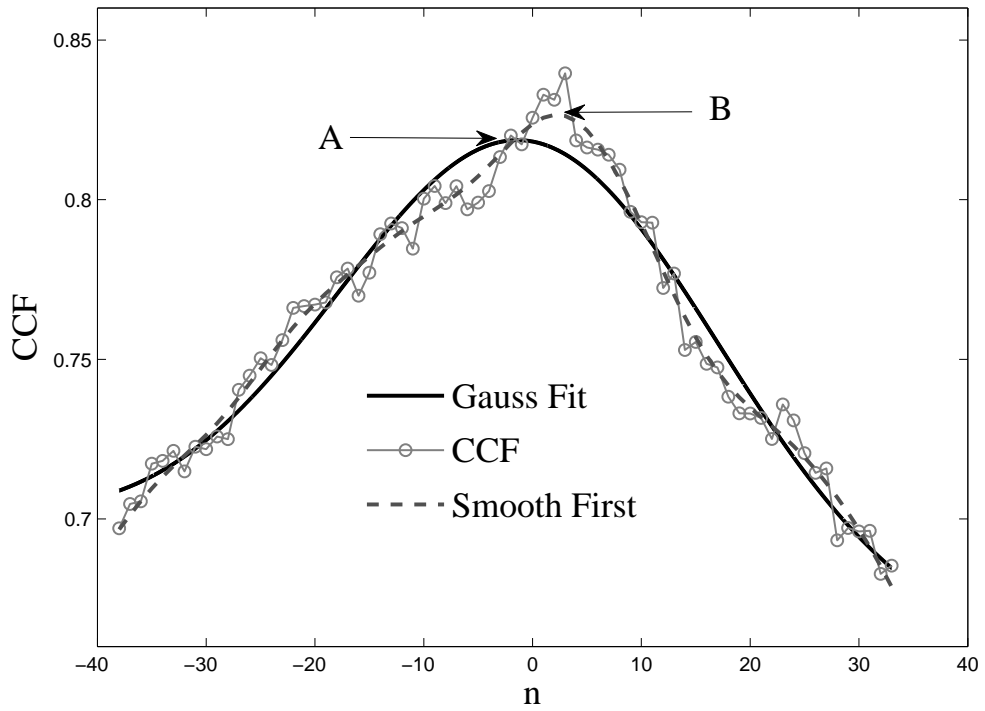


Fig. 5.— A comparison between Gaussian fitting and loess filter methods for GRB 071020. A and B indicate the maximums of the CCF smoothed by Gaussian function and loess smooth method, respectively.

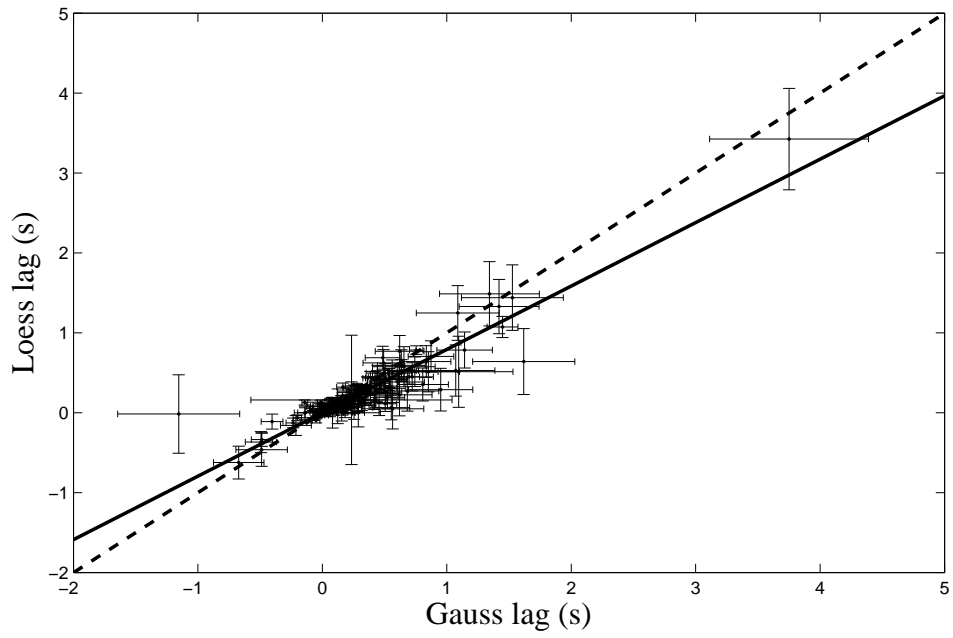


Fig. 6.— $\log_{\text{Gauss}} - \log_{\text{loess}}$ relation. The solid line shows the best fit between \log_{Gauss} and \log_{loess} . The dashed line displays the diagonal. The 1σ simulation uncertainties are used for error bars.

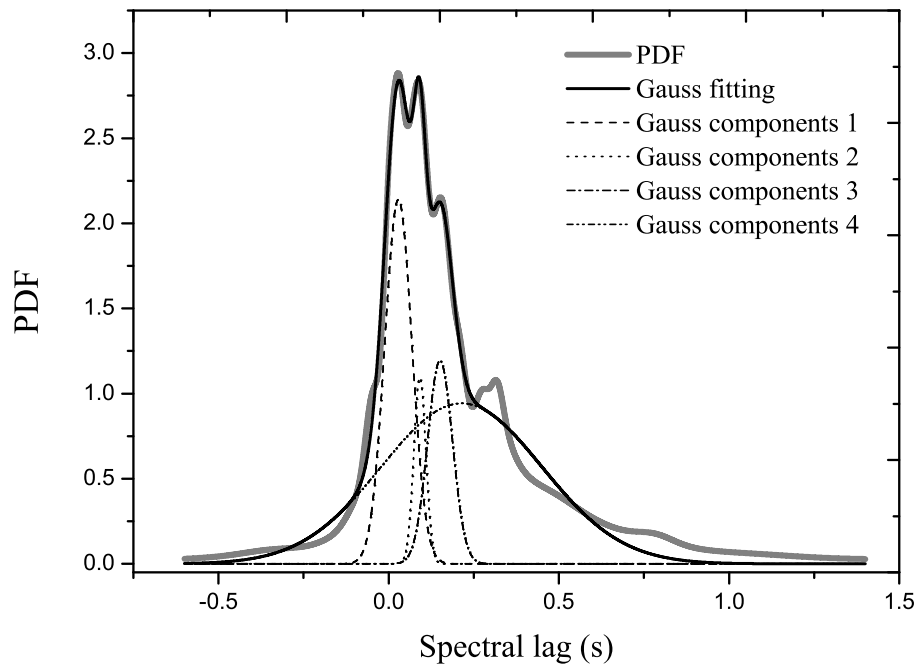


Fig. 7.— The PDF of loess spectral lags. The PDF is fitted by four Gauss components which locate 0.028 ± 0.001 s (dashed line), 0.091 ± 0.003 s (dotted line), 0.15 ± 0.01 s (dash-dot line), and 0.21 ± 0.01 s (dash-dot-dot line), respectively.

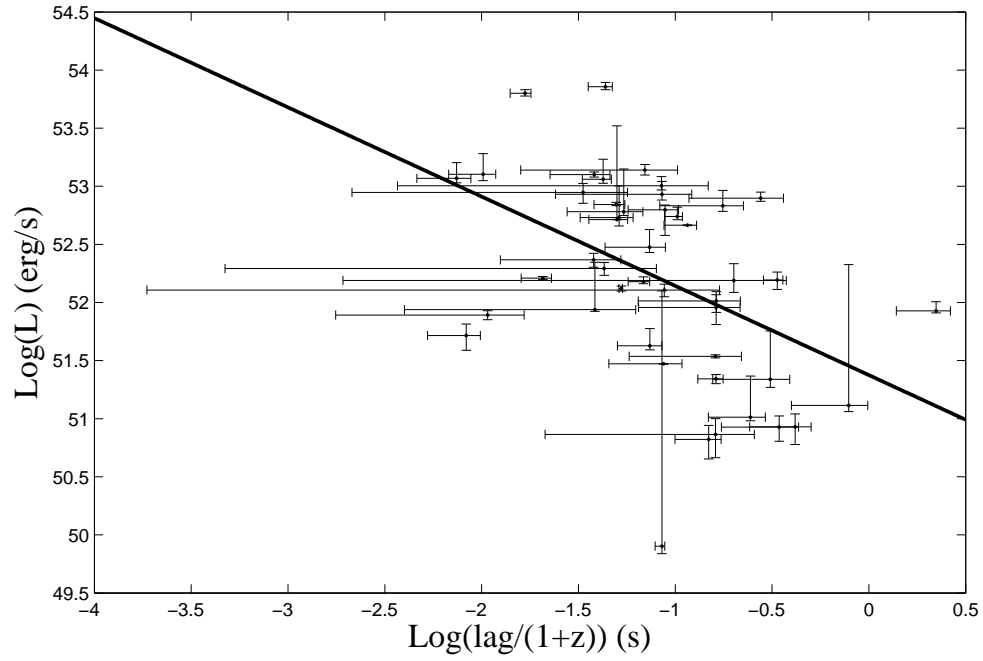


Fig. 8.— The log-log relation between isotropic luminosity and spectral lag. The factor $(1+z)^{-1}$ corrects for the time dilation effect.

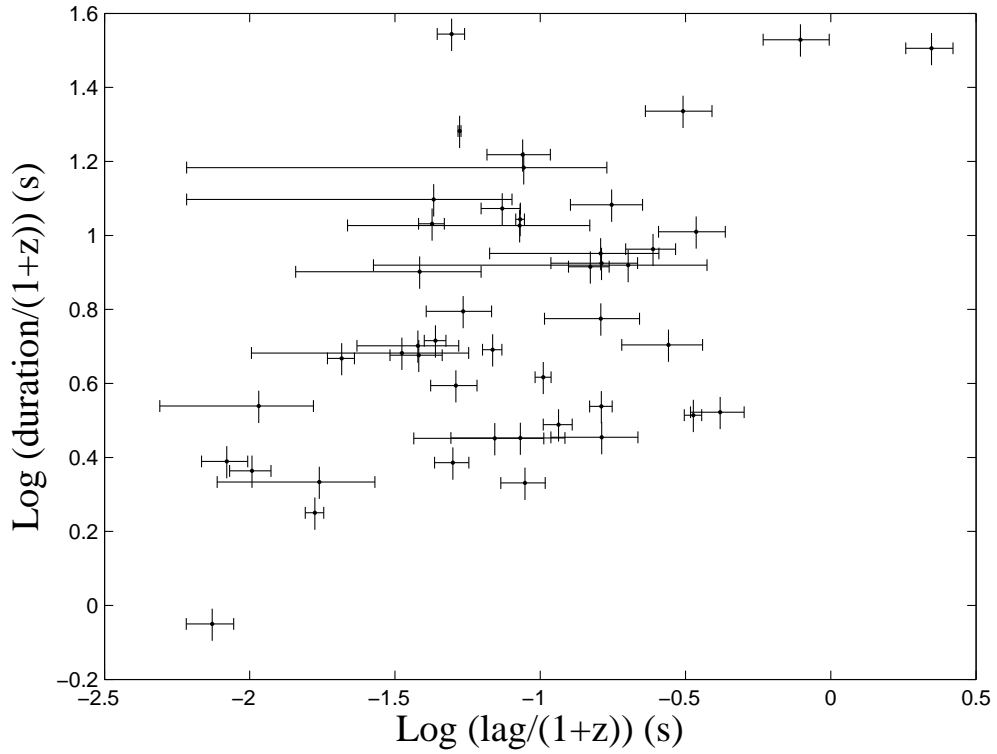


Fig. 9.— Lag-pulse duration relation in the rest frame of GRBs. Both axes are in units of second. The factor $(1+z)^{-1}$ corrects for the time dilation effect. Each duration error is set as 10% of its value.

Table 1. The spectral lags of GRB with measured redshift.

GRB	Peak No.	Start time	Stop time	$\text{lag}_{\text{Gauss}}$	$\text{lag}_{\text{Smooth}}(\text{s})$ $\alpha = 0.1$	$\text{lag}_{\text{Smooth}}$ $\alpha = 0.05$
(1)	(2)	(s) (3)	(s) (4)	(s) (5)	(s) (6)	(s) (7)
050318		24.52	32.392	0.06 ± 0.05	0 ± 0.05	0.11 ± 0.06
050401		22.968	33.992	0.44 ± 0.1	0.27 ± 0.13	0.14 ± 0.05
050416A		-1.648	3.856	0.49 ± 0.1	0.69 ± 0.14	0.64 ± 0.1
050603		-3.24	3.560	0.06 ± 0.02	0.06 ± 0.02	0.05 ± 0.02
050922C		-3.624	4.152	0.21 ± 0.02	0.16 ± 0.02	0.27 ± 0.11
051111		-8.88	12.304	1.1 ± 0.4	0.51 ± 0.44	0.48 ± 0.2
060206		-1.976	8.856	0.44 ± 0.07	0.45 ± 0.08	0.43 ± 0.2
060210		-5.032	9.304	0.51 ± 0.2	0.43 ± 0.2	0.34 ± 0.1
060418		23.104	34.848	0.08 ± 0.2	0 ± 0.2	0.02 ± 0.02
060526		-5.040	16.192	0.25 ± 0.06	0.16 ± 0.06	0.21 ± 0.08
060614		-5.360	7.072	0.08 ± 0.02	0.1 ± 0.02	0.08 ± 0.02
060814	1	-0.696	29.704	0.33 ± 0.04	0.16 ± 0.04	0.19 ± 0.09
	2	58.6	91.192	-0.49 ± 0.1	-0.34 ± 0.13	-0.6 ± 0.4
060904B		-11.488	25.424	0.64 ± 0.1	0.53 ± 0.14	0.58 ± 0.2
060912		-1.2	4.768	0.24 ± 0.03	0.22 ± 0.03	0.22 ± 0.04
060927	1	-1.864	3.896	0.06 ± 0.02	0.05 ± 0.02	0.08 ± 0.02
	2	3.48	8.600	-0.02 ± 0.01	0 ± 0.02	0.21 ± 0.1
	3	13.16	29.064	-0.67 ± 0.2	-0.62 ± 0.2	-0.74 ± 0.3
061007	1	-4.296	19.768	0.52 ± 0.1	0.19 ± 0.14	0.18 ± 0.05
	2	24.072	41.176	0.18 ± 0.06	0.16 ± 0.06	0.11 ± 0.05
	3	41.592	65.928	0.17 ± 0.02	0.16 ± 0.02	0.16 ± 0.01
061121	1	-3.112	8.6	0.84 ± 0.2	0.64 ± 0.2	0.82 ± 0.3
	2	58.712	82.312	0.02 ± 0.02	0.03 ± 0.02	0.03 ± 0.02
061201		-5.576	7.976	0.2 ± 0.03	0.19 ± 0.03	0.08 ± 0.02
070306		88.944	108.848	0.16 ± 0.06	0.1 ± 0.06	-0.08 ± 0.06
070508		-5.712	29.12	0.09 ± 0.02	0.1 ± 0.02	0.1 ± 0.02
070521	1	7.3520	28.312	0.32 ± 0.06	0.26 ± 0.06	0.18 ± 0.04
	2	28.792	33.48	0.29 ± 0.03	0.14 ± 0.03	0.11 ± 0.02

Table 1—Continued

GRB	Peak No.	Start time	Stop time	$\text{lag}_{\text{Gauss}}$	$\text{lag}_{\text{Smooth}}(\text{s})$ $\alpha = 0.1$	$\text{lag}_{\text{Smooth}}$ $\alpha = 0.05$
(1)	(2)	(s) (3)	(s) (4)	(s) (5)	(s) (6)	(s) (7)
	3	33.416	40.232	0.08 ± 0.01	0.1 ± 0.01	0.14 ± 0.07
070714B		-1.728	2.976	0.02 ± 0.02	0.02 ± 0.02	0.02 ± 0.02
070810A		-6.872	12.008	0.74 ± 0.2	0.51 ± 0.2	0.5 ± 0.3
071003		-2.656	29.92	0.51 ± 0.09	0.11 ± 0.1	0.11 ± 0.04
071010B		-2.264	20.76	0.19 ± 0.02	0.14 ± 0.02	0.14 ± 0.05
071020		-3.808	3.456	-0.02 ± 0.02	0.03 ± 0.02	0.03 ± 0.02
071117		-1.392	6.224	0.75 ± 0.05	0.78 ± 0.05	0.78 ± 0.06
080210		-6.928	23.712	0.64 ± 0.2	0.59 ± 0.2	0.53 ± 0.3
080319B		-5.792	62.032	0.2 ± 0.02	0.1 ± 0.01	0.35 ± 0.02
080319C		-2.784	15.6	0.23 ± 0.04	0.16 ± 0.04	0.19 ± 0.08
080330		-2.432	15.264	0.16 ± 0.05	0.32 ± 0.05	0.03 ± 0.02
080411	1	14.960	23.36	0.3 ± 0.02	0.21 ± 0.01	0.2 ± 0.02
	2	38.720	49.04	0.2 ± 0.02	0.18 ± 0.02	0.18 ± 0.02
	3	52.608	62.624	0.29 ± 0.2	0 ± 0.2	0 ± 0.2
	4	62.512	72.192	0.23 ± 0.8	0.16 ± 0.1	0.11 ± 0.1
080413A	1	-2.888	10.6	0.2 ± 0.03	0.18 ± 0.03	0.18 ± 0.05
	2	12.104	33.72	-0.05 ± 0.03	-0.1 ± 0.03	-0.11 ± 0.06
	3	35.032	58.264	0.66 ± 0.3	0.58 ± 0.25	-0.05 ± 0.1
080413B		-2.576	7.744	0.14 ± 0.02	0.14 ± 0.02	0.13 ± 0.02
080430		-1.288	14.936	0.42 ± 0.08	0.43 ± 0.08	0.51 ± 0.2
080603B	1	-1.176	6.776	-0.2 ± 0.03	-0.06 ± 0.04	-0.03 ± 0.02
	2	6.6	19.688	0.38 ± 0.06	0.27 ± 0.06	0.37 ± 0.1
	3	38.872	74.04	0.29 ± 0.08	0.27 ± 0.08	0.19 ± 0.08
080605		-6.84	21.544	0.12 ± 0.02	0.11 ± 0.02	0.11 ± 0.01
080607		-7.296	13.664	0.16 ± 0.02	0.18 ± 0.02	0.14 ± 0.01
080707		-11.864	10.952	0.62 ± 0.2	0.77 ± 0.2	1.12 ± 0.5
080810		-17.824	43.008	-0.03 ± 0.02	0 ± 0.02	0 ± 0.02
080916A		-7.568	49.52	1.42 ± 0.3	1.33 ± 0.3	1.25 ± 0.4

Table 1—Continued

GRB	Peak No.	Start time	Stop time	lag _{Gauss}	lag _{Smooth} (s) $\alpha = 0.1$	lag _{Smooth} $\alpha = 0.05$
(1)	(2)	(s) (3)	(s) (4)	(s) (5)	(s) (6)	(s) (7)
080928		195.432	225.016	-0.08 ± 0.05	0.08 ± 0.05	0.08 ± 0.03
081203A		-0.224	47.056	0.68 ± 0.2	0.3 ± 0.2	0.3 ± 0.1
081222		-1.888	16.000	0.31 ± 0.02	0.14 ± 0.03	0.14 ± 0.02
090423		-12.84	30.936	0.39 ± 0.2	0.30 ± 0.2	0.24 ± 0.1
090424	1	-1.784	5.4	0.01 ± 0.02	0.03 ± 0.02	0.03 ± 0.02
	2	5.656	26.616	0.08 ± 0.08	0.11 ± 0.08	0.08 ± 0.07
090510		-1.888	6.4	0.03 ± 0.02	0 ± 0.01	0 ± 0.02
090618	1	-7.568	41.776	3.75 ± 0.6	3.42 ± 0.6	3.4 ± 0.9
	2	51.2	72.224	0.46 ± 0.03	0.3 ± 0.05	0.3 ± 0.1
	3	72.112	99.52	0.001 ± 0.02	0 ± 0.02	0 ± 0.02
	4	99.088	140.384	0.55 ± 0.1	0.3 ± 0.1	0.3 ± 0.2
090715B	1	-13.952	34.432	0.87 ± 0.2	0.7 ± 0.2	0.4 ± 0.2
	2	48.56	89.2	0.61 ± 0.2	0.38 ± 0.2	0.53 ± 0.3
091018		-1.112	5.688	0.35 ± 0.03	0.32 ± 0.03	0.32 ± 0.05
091127	1	-1.2	3.952	0.02 ± 0.01	0.02 ± 0.02	0.02 ± 0.02
	2	4.928	11.856	0.04 ± 0.03	0 ± 0.02	0.03 ± 0.05
091208B	1	-1.088	4.784	0.36 ± 0.1	0.34 ± 0.1	0.34 ± 0.1
	2	5.328	17.904	0.07 ± 0.02	0.06 ± 0.02	0.03 ± 0.02
100316B		-6.696	12.792	0.81 ± 0.2	0.35 ± 0.2	0.34 ± 0.1

Note. — col.(1): The GRB trigger number. Col.(2): The peak number of GRB. Col.(3): The start time of individual pulse relative to the GRB trigger time. Col.(4): The stop time of individual pulse relative to the GRB trigger time. Col.(5): The spectral lags plus errors between 15-25 keV and 50-100 keV by fitting with Gaussian plus linear equation. Col.(6): The spectral lags plus errors calculated by smooth method with $\alpha = 0.1$. Col.(7): The spectral lags plus errors calculated by smooth method with $\alpha = 0.05$.

Table 2. The spectral lags of GRB with unknown redshift.

GRB	Peak No.	Start time	Stop time	$\text{lag}_{\text{Gauss}}$	$\text{lag}_{\text{Smooth}}(\text{s})$ $\alpha = 0.1$	$\text{lag}_{\text{Smooth}}$ $\alpha = 0.05$
(1)	(2)	(s) (3)	(s) (4)	(s) (5)	(s) (6)	(s) (7)
041220		-2.608	8.096	0.21 ± 0.05	0.08 ± 0.05	0.18 ± 0.08
041224		16.032	41.568	0.49 ± 0.2	0.62 ± 0.2	0.77 ± 0.4
050124		-6.264	6.904	0.03 ± 0.02	0.08 ± 0.02	0.05 ± 0.02
050219B	1	-6.376	5.432	0.23 ± 0.06	0.05 ± 0.06	0.03 ± 0.02
	2	-5.976	15.896	0.32 ± 0.05	0.29 ± 0.05	0.10 ± 0.03
050326	1	-2.736	13.392	0.03 ± 0.02	0.02 ± 0.02	0.02 ± 0.02
	2	15.52	30.560	0.09 ± 0.02	0.06 ± 0.02	0.06 ± 0.02
050418		-25.416	31.000	0.44 ± 0.09	0.50 ± 0.1	0.42 ± 0.2
050509A		-8.664	8.680	0.06 ± 0.03	0.14 ± 0.04	0.06 ± 0.02
050701		2.968	13.384	0.21 ± 0.05	0.14 ± 0.06	0.29 ± 0.2
050717	1	-1.136	16.672	0.01 ± 0.02	0.05 ± 0.02	0.03 ± 0.02
	2	16.368	39.408	0.46 ± 0.2	0.13 ± 0.2	0.10 ± 0.03
050801		-2.464	9.9680	0.29 ± 0.08	0.10 ± 0.09	0.00 ± 0.02
050820B	1	-1.608	5.3840	0.42 ± 0.2	0.24 ± 0.2	0.11 ± 0.03
	2	5.2240	17.688	-0.40 ± 0.09	-0.11 ± 0.09	-0.21 ± 0.07
051016B	1	-0.584	2.056	0.26 ± 0.08	0.14 ± 0.07	0.13 ± 0.07
	2	2.056	7.480	-0.49 ± 0.2	-0.46 ± 0.2	-1.07 ± 0.6
060105	1	-12.00	18.856	0.43 ± 0.09	0.16 ± 0.1	0.16 ± 0.05
	2	19.256	43.368	0.55 ± 0.2	0.06 ± 0.2	0.06 ± 0.02
060110		-2.104	14.248	1.09 ± 0.3	1.25 ± 0.3	1.34 ± 0.6
060111A		-7.456	18.608	1.53 ± 0.4	1.44 ± 0.4	1.95 ± 0.5
060117	1	-2.776	5.176	0.12 ± 0.02	0.08 ± 0.02	0.08 ± 0.02
	2	5.5760	18.936	0.08 ± 0.02	0.03 ± 0.02	0.03 ± 0.02
060223B		-7.840	8.400	-1.15 ± 0.5	-0.02 ± 0.5	0.03 ± 0.02
060306		-3.584	8.320	0.18 ± 0.02	0.08 ± 0.03	0 ± 0.02
060313		-3.024	2.048	0 ± 0.02	0 ± 0.02	0 ± 0.02
060428A		-3.136	11.904	0.18 ± 0.06	0.00 ± 0.06	0.05 ± 0.02
060708		-1.976	10.392	0.95 ± 0.3	0.29 ± 0.3	0.29 ± 0.1

Table 2—Continued

GRB	Peak No.	Start time	Stop time	$\text{lag}_{\text{Gauss}}$	$\text{lag}_{\text{Smooth}}(\text{s})$ $\alpha = 0.1$	$\text{lag}_{\text{Smooth}}$ $\alpha = 0.05$
(1)	(2)	(s) (3)	(s) (4)	(s) (5)	(s) (6)	(s) (7)
060719	1	-0.888	13.352	0.85 ± 0.3	0.51 ± 0.3	0.5 ± 0.2
	2	40.136	60.168	0.51 ± 0.1	0.26 ± 0.1	0.32 ± 0.1
060813		-0.888	11.192	-0.01 ± 0.02	0.03 ± 0.02	0.03 ± 0.02
060825		-4.272	8.016	0.54 ± 0.1	0.43 ± 0.1	0.45 ± 0.2
060904A		41.336	81.256	-0.02 ± 0.02	0.1 ± 0.02	0.1 ± 0.04
061004		-0.008	11.512	-0.01 ± 0.03	0.13 ± 0.03	0.13 ± 0.04
061021		0	10.880	0.03 ± 0.02	0 ± 0.02	0 ± 0.02
061126		2.488	14.920	0.14 ± 0.03	0.13 ± 0.03	0.24 ± 0.1
061202		70.648	95.976	-0.14 ± 0.06	0 ± 0.06	0 ± 0.07
061222A	1	23.184	39.984	-0.23 ± 0.06	-0.13 ± 0.06	0.03 ± 0.02
	2	45.040	72.672	0.26 ± 0.08	0.00 ± 0.08	-0.1 ± 0.09
	3	77.472	99.824	0.14 ± 0.02	0.14 ± 0.02	0.14 ± 0.02
070220		-3.512	27.928	-0.05 ± 0.02	-0.06 ± 0.02	-0.05 ± 0.02
070427		-3.032	17.864	1.62 ± 0.4	0.64 ± 0.4	0.26 ± 0.1
070714A		-1.176	8.024	0.34 ± 0.2	0.27 ± 0.2	0.22 ± 0.3
070911	1	7.496	28.984	-0.14 ± 0.08	0 ± 0.08	0 ± 0.02
	2	27.768	62.776	0.32 ± 0.03	0.30 ± 0.03	0.24 ± 0.06
070917		-1.128	9.432	0.25 ± 0.02	0.21 ± 0.02	0.21 ± 0.02
080229A	1	-9.240	12.408	1.07 ± 0.31	0.53 ± 0.3	0.45 ± 0.2
	2	24.744	52.040	0.30 ± 0.02	0.32 ± 0.02	0.22 ± 0.03
080328	1	-12.176	54.848	0.62 ± 0.26	0.22 ± 0.3	0.16 ± 0.08
	2	65.744	101.824	0.70 ± 0.08	0.45 ± 0.09	0.48 ± 0.2
080409	1	-2.088	6.552	0.23 ± 0.05	0.34 ± 0.05	0.35 ± 0.2
	2	5.960	13.336	0.09 ± 0.03	0.00 ± 0.03	0.08 ± 0.04
080426		-1.376	3.232	0.10 ± 0.01	0.08 ± 0.02	0.08 ± 0.02
080613B		-7.784	34.680	0.05 ± 0.01	0.03 ± 0.02	0.03 ± 0.02
080701		-5.096	7.336	1.34 ± 0.40	1.49 ± 0.4	1.58 ± 0.5
080714		-4.000	6.752	0.53 ± 0.14	0.42 ± 0.1	0.16 ± 0.3

Table 2—Continued

GRB	Peak No.	Start time	Stop time	$\text{lag}_{\text{Gauss}}$	$\text{lag}_{\text{Smooth}}(\text{s})$ $\alpha = 0.1$	$\text{lag}_{\text{Smooth}}$ $\alpha = 0.05$
(1)	(2)	(s) (3)	(s) (4)	(s) (5)	(s) (6)	(s) (7)
080727B	1	-0.368	4.928	-0.05 ± 0.02	-0.05 ± 0.02	-0.06 ± 0.02
	2	5.408	11.152	0.07 ± 0.02	0.08 ± 0.02	0.06 ± 0.02
080727C		-9.032	52.120	0.36 ± 0.1	0.34 ± 0.1	0.37 ± 0.2
080915B		-0.768	2.416	-0.04 ± 0.02	-0.05 ± 0.02	-0.05 ± 0.03
081210		6.720	23.120	0.05 ± 0.07	0.10 ± 0.07	0.05 ± 0.02
090113	1	-3.072	3.376	0.20 ± 0.04	0.10 ± 0.04	0.19 ± 0.09
	2	3.264	5.328	0.16 ± 0.05	0.02 ± 0.05	0.05 ± 0.02
	3	4.928	12.176	0.15 ± 0.1	0.11 ± 0.1	0.19 ± 0.1
090129		-3.472	23.872	0.46 ± 0.08	0.37 ± 0.08	0.30 ± 0.1
090201		-4.256	3.920	0.12 ± 0.2	0.08 ± 0.2	0.13 ± 0.1
090201		4.736	15.888	0.56 ± 0.2	0.50 ± 0.2	0.70 ± 0.3
090301A	1	-6.352	14.336	0.32 ± 0.08	0.11 ± 0.08	0.11 ± 0.02
	2	14.464	19.440	0.16 ± 0.04	0.21 ± 0.04	0.22 ± 0.05
	3	21.104	28.784	0.15 ± 0.02	0.11 ± 0.02	0.11 ± 0.02
	4	29.872	37.584	0.07 ± 0.02	0.06 ± 0.02	0.06 ± 0.02
090401B	1	-0.448	6.288	0.11 ± 0.02	0.06 ± 0.02	0.06 ± 0.02
	2	6.192	13.104	0.10 ± 0.02	0.03 ± 0.02	0.03 ± 0.02
090404	1	14.928	36.528	0.19 ± 0.04	0.05 ± 0.05	0.11 ± 0.06
	2	33.504	45.600	-0.21 ± 0.1	-0.16 ± 0.1	0.08 ± 0.1
090518		-5.888	3.904	-0.14 ± 0.02	0.13 ± 0.03	0.11 ± 0.03
090530		-3.024	7.808	0.02 ± 0.03	0.10 ± 0.03	0.06 ± 0.03
090709A	1	-21.712	18.512	0.27 ± 0.05	0.27 ± 0.05	0.19 ± 0.06
	2	18.032	66.400	0.09 ± 0.02	0.16 ± 0.02	0.16 ± 0.04
090813	1	-0.952	3.208	0.02 ± 0.02	0.00 ± 0.02	0.05 ± 0.02
	2	5.384	9.304	0.16 ± 0.1	0.00 ± 0.1	0.06 ± 0.07
090929B		-9.064	53.800	0.28 ± 0.08	0.29 ± 0.08	0.18 ± 0.06
091020		-7.136	23.568	-0.02 ± 0.05	0.00 ± 0.05	0.37 ± 0.2
100111A		-5.512	11.752	0.27 ± 0.07	0.26 ± 0.08	0.29 ± 0.1

Table 2—Continued

GRB	Peak No.	Start time	Stop time	$\text{lag}_{\text{Gauss}}$	$\text{lag}_{\text{Smooth}}(\text{s})$ $\alpha = 0.1$	$\text{lag}_{\text{Smooth}}$ $\alpha = 0.05$
(1)	(2)	(s) (3)	(s) (4)	(s) (5)	(s) (6)	(s) (7)
100423A		-3.992	4.552	0.06 ± 0.02	0.03 ± 0.02	0.03 ± 0.02
100522A	1	-2.184	7.752	-0.09 ± 0.02	0.03 ± 0.02	0.03 ± 0.02
	2	23.432	39.672	0.56 ± 0.3	0.05 ± 0.3	0.24 ± 0.5
100615A	1	-1.60	9.120	0.62 ± 0.1	0.51 ± 0.1	0.51 ± 0.08
	2	8.976	22.784	0.35 ± 0.07	0.16 ± 0.07	0.16 ± 0.04
	3	22.496	48.992	-0.49 ± 0.08	-0.34 ± 0.09	-0.5 ± 0.2
100619A	1	-7.824	16.592	0.28 ± 0.05	0.06 ± 0.05	-0.02 ± 0.02
	2	79.648	99.792	0.03 ± 0.02	-0.03 ± 0.02	0.06 ± 0.03
100621A		-3.288	42.088	1.45 ± 0.1	1.07 ± 0.13	1.07 ± 0.1
100704A		-9.032	25.512	1.14 ± 0.2	0.78 ± 0.23	1.04 ± 0.4
100816A		-1.360	4.176	0.12 ± 0.02	0.10 ± 0.01	0.10 ± 0.02
100906A	1	-3.248	21.616	0.50 ± 0.04	0.34 ± 0.05	0.27 ± 0.05
	2	93.024	131.408	0.72 ± 0.2	0.45 ± 0.18	0.5 ± 0.2

Note. — Each Column represents the same as table 1.